

Chapter 28

Formation and Properties of Silk Thin Films

Wayne S. Muller, Lynne A. Samuelson, Stephen A. Fossey, and
David Kaplan

Biotechnology Division, Natick Research, Development, and Engineering
Center, U.S. Army, Natick, MA 01760-5020

As an immobilization matrix cast fibroin silk films exhibit useful properties including stability to most solvents, biological compatibility, phase transition for the physical entrapment of reactive molecules, and the capability to retain high activity of the entrapped molecules. However, in the casting process there is limited control over the density, thickness and the orientation of the polymer chains. The Langmuir-Blodgett (LB) technique can enhance the control of the membrane structure and allow improved control over membrane properties. We have formed natural silk films using the Langmuir technique. Silk fibroin, regenerated from *Bombyx mori* cocoons, formed stable LB thin films as indicated from pressure/area isotherms. Multiple layers of the silk fibroin were deposited on a number of substrates and basic information about the physical properties of the LB films were obtained with transmission electron microscopy (TEM) and ellipsometry data. Preliminary analysis of electron diffraction data from the film indicates a polycrystalline structure consistent with the known structure of silk. Infrared spectrometric analysis of these silk films using attenuated total reflectance (ATR) gave wavenumbers for amide I, II, III and V bands, which are in agreement with the silk II conformation reported for cast silk membranes.

Over the centuries, silk has been valued as a textile fiber because of its strength, elasticity, softness, lustre, absorbency and affinity for dyes. *Bombyx mori* silk consists of two types of proteins, fibroin and sericin. Fibroin is the protein that forms the filaments of silkworm silk and gives silk its unique physical and chemical properties. Sericins are the group of gummy proteins which bind the fibroin filaments. Silk fibroin can be used in

various forms, such as gels, powders, fibers, or membranes, depending on application. Recently (1-5) silk fibroin has been used as an immobilization matrix for enzymes. As a biomaterial it has many advantages over both natural and synthetic materials used in biosensor systems. These attributes include its biological compatibility, stability to most solvents including water and good tensile strength and elasticity properties. Our interests lie in the membrane properties of silk and the utilization of the phase transition (silk I to silk II) in the processing of water-soluble fibroin polymer to water-insoluble films.

Fibroin contains a unique amino acid composition and primary structure (6,7). Its major advantage as an enzyme immobilization matrix is that it entraps the enzyme. This entrapment of the enzyme without the usual cross-linking chemicals alleviates the problems of residual cross-linking chemicals in the matrix, which can deactivate the enzyme and the chemical cross-linking, which can negatively impact enzyme activity. The entrapment process is accomplished by physical, chemical or mechanical treatment of the membrane (e.g., change in temperature, pH, solvent, mechanical shear or stretch), which induces a phase transition. The phase transition is a conformational change of the protein from mostly a random coil to a β sheet conformation entrapping the reactive molecule. *Bombyx mori* silk fibroin has been used as an immobilization matrix for enzymes such as glucose oxidase (1-4), alkaline phosphatase (8), peroxidase (5), and invertase (9).

Silk fibroin exhibits at least three conformations: random coil, silk I, and silk II. All three conformations can be formed by the appropriate preparation conditions and each is interchangeable under certain conditions (10). Silk structures studied for phase transitions as immobilization matrices have in the past been in the form of cast membranes. The cast silk membranes have good properties as membrane materials; however, the casting process has limitations. There is limited control over the thickness of the membrane or the density and the orientation of the polymer chains. Since the functionality of these membranes, including permeability, the activity of entrapped enzymes, and mechanical integrity, is dependent in part on conformation, density, and orientation of the polymer chains, new processing techniques to control these properties would be useful. The Langmuir-Blodgett (LB) technique is used in this study in an attempt to enhance the control of the physical processing of silk fibroin protein. This enhanced control could therefore provide new opportunity for these membranes as immobilization matrices and in other barrier and biomaterial applications.

We describe the formation and characterization of natural silk fibroin films using the LB technique. Basic information regarding the physical characteristics of the thin films is obtained from pressure-area isotherms, electron micrographs, and ellipsometry. Analysis of the silk fibroin LB films with infrared spectroscopy and electron diffraction provides insight into the silk conformation favored at ambient temperature and the expected polycrystalline order of the silk film.

Experimental

B. mori cocoon silk was regenerated using 9.3M LiBr solution and dialyzed for three days in distilled water. A Pasteur pipet was used to apply the solubilized silk to a Lauda Filmbalance FW2 (Brinkmann Instr. Inc., Westbury, NY). To generate pressure/area isotherms, the silk fibroin was added to the surface of a Milli Q water subphase at 24° C and the barrier compressed at a rate of 46 cm²/min (approximately 125 mg of silk was added to form isotherm in Figure 1). Transmission Electron Microscopy (TEM) was performed on the films using a Hitachi H 600 (Rockville, MD) with samples collected from the surface of the trough using T 1000 grids. Fourier Transform Infrared Reflectance (FTIR) Attenuated Total Reflection (ATR) analysis was performed on a Nicolet 20SXB Infrared Spectrometer (Madison, WI) with an accessory holder for ATR (Harrick Scientific Co., Ossining, NY). Thin film samples for FTIR analysis were transferred and collected on germanium prisms at a pressure of 16.7 mN/m, a dipping speed of 0.2 cm/min and a temperature of 20° C. The silk films were deposited on frosted glass slides under the same conditions used for the FTIR samples. These films were analyzed on a Thin Film Ellipsometer Type 43603-200E (Rudolph Research, Flanders, NJ) to determine the thickness of the transferred material.

Results & Discussion

Figure 1 is a typical pressure/area isotherm of the soluble silk. The steep slope and smooth appearance of the curve indicate the formation of a stable film. It should be noted that the x-axis of the isotherm is in arbitrary units because the silk fibroin has an estimated molecular weight of 350 kDa to 415 kDa (11), which exceeds the limits of the Lauda software program. A molecular weight of 75.53 Da was used as the basis of standardizing the calculation for the x-axis units, derived from the amino acid composition of fibroin (12,13) and is based on the average weight of each amino acid monomer in the silk fibroin polymer. It remains difficult to obtain an accurate quantitation of the area per molecule in the stabilized film due to the complex secondary structure of the silk fibroin protein.

Silk fibroin does not exhibit the typical amphiphathic character of LB materials suitable for monolayer formation. Also, silk fibroin exhibits unique solubility characteristics (7,14), which can make the material difficult to work with in an LB system. Silk fibroin is insoluble in volatile nonpolar solvents often used in the application of surfactants to an aqueous subphase. Silk fibroin is also insoluble in dilute acids and alkali, and resistant to most proteolytic enzymes (11,15), but soluble in 9.3M LiBr aqueous solution. After dialysis, the solubilized silk fibroin remains in solution if undisturbed. After application to the trough, a portion of the polymer enters the aqueous subphase and the remainder sits at the air-water interface. This event is evident from the protein residue observed when cleaning the trough. This

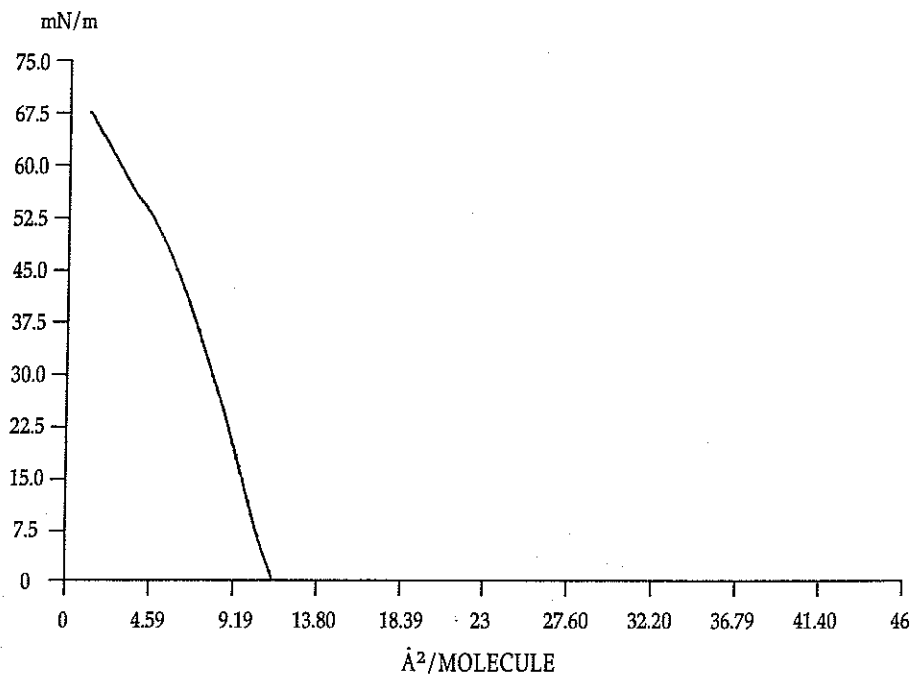


Figure 1. Typical pressure/area isotherm of solubilized silk fibroin at 24° C.

unusual solubility behavior adds to the difficulty in obtaining an accurate determination of the area per polymer chain.

The silk fibroin films demonstrate excellent stability and transfer properties, indicative of a well-behaved Langmuir-Blodgett system. The compression barrier has been stabilized for half hour to hour time periods at various pressures (10, 15, 20, 25, 30, 35 mN/m) with no indication of film collapse. Films remained stable overnight (16 h) without a change in area when studied at our usual working pressure for transfer at 16.7 mN/m. In Figure 1, a typical isotherm for silk, there is no sudden drop in surface pressure with compression, which would be indicative of a collapsed film. The steady rise in surface pressure of the isotherm indicates the increasing resistance to dense molecular packing. Upon complete collapse of the film, it is possible to remove very long fibers with the tip of a pipet.

Table I presents the ellipsometry data for silk films indicating the relative thickness of a transferred LB silk film. Many biomolecular materials exhibit Y or Z type deposition (16). For Y deposition on a hydrophilic surface the first monolayer is transferred as the substrate is raised through the subphase. Subsequently a monolayer is deposited on each traversal of the surface. With Z deposition material transfer occurs only on movement of substrate up through the monolayer. We believe that Y type deposition is characteristic of the silk fibroin thin film based on our observations of the change in area and shape of the meniscus at the air/water interface during vertical deposition. The average thickness of a monolayer determined from the data in Table I was approximately 11.6 to 11.9 Å. The ellipsometry data indicated that the average thickness increased with the number of layers deposited. The increased average thickness maybe due to a combination of factors, the inefficient packing of layers with increasing numbers and/or the nonuniformity of the layers. Therefore, by extrapolation back to a single layer, a average value of 11.6 to 11.9 Å was established.

Silk from *B. mori* consists of antiparallel β sheets as first described by Marsh et al. (17). The fibroin consists of both crystalline (short side-chain amino acid monomers glycine, alanine, serine) and amorphous (amino acids with bulkier side chains) domains. There have been two types of crystalline structures proposed for silk, silk I and silk II. For silk II, the insoluble and more stable form of silk, the reported unit cell based on X-ray diffraction data has an interchain distance of 9.4 Å, a fiber axis distance of 6.97 Å, and an intersheet distance of 9.2 Å (17). The silk does not exhibit the typical amphipathic character of LB materials thus the polymer chains at the air/water interface are probably parallel to the surface. A single chain of silk crystalline domain is 4.5 to 4.7 Å thick while the amorphous chains vary in their thickness. It maybe in forming the silk LB film the nonaqueous soluble silk II (crystalline domains) are at the air/water interface and the soluble amorphous domains are buckled into the subphase. Such a model of the film structure on the surface would be consistent with the ellipsometry value of 11.6 to 11.9 Å and the increase in average thickness of the layers. The amorphous domains would not be uniform in their arrangement underneath the crystalline domains creating an irregular surface with the ellipsometry value representing the average thickness of the silk film deposited on the substrate.

Silk I is also of interest due to its metastable nature, its role in the natural processing of silk, and its unresolved structure. Silk I is the conformation of the soluble form of silk fibroin that rapidly undergoes a phase transition to the insoluble silk II conformation (11,18). This transition can be activated by mechanical agitation, exposure to hydrophilic organic solvents, or temperature changes (19-23). Due to this instability, experimental studies with silk I have been primarily on samples of low orientation (attempts to improve orientation result in conversion to silk II). Therefore, elucidation of the structure of silk I has depended on molecular modeling and comparisons with the limited available experimental evidence (11). A number of models have been proposed, including the Lotz and Keith [24] crankshaft model based on poly(L Ala-Gly) lamellar crystals (intersheet distance of 14.4 Å) and a recent model of Fossey et al. (18) based on conformational energy calculations with copolymers of Gly-Ala and stacked sheets (intersheet distance of 11.3 Å).

Infrared spectroscopy was used to partially characterize the structure of silk in the LB film. Yoshimizu and Asakura (25), in a study on cast films with a thickness of 100-250 µm, employed FTIR (ATR) to determine the conformational transition of the silk membrane surface treated with methanol. The absorption bands observed for membranes treated with methanol had wavenumbers of 1625 (amide I), 1528 (amide II), and 1260 cm^{-1} (amide III), characteristic of a silk II structure. Membranes without methanol treatment showed absorption bands at 1650 (amide I), 1535 (amide II), and 1235 cm^{-1} (amide II), which were assigned the random coil conformation. In addition, Asakura et al. [26] observed that the amide V band had a frequency of 700 cm^{-1} for silk II compared to a 650 cm^{-1} for the random coil conformation.

Table II compares the FTIR wavenumbers for cast membranes (silk I, silk II) with results obtained on silk fibroin LB films. A total of eleven silk layers were deposited on a germanium prism. Absorption bands were observed at 1624 (amide I), 1522 (amide II), 1258 cm^{-1} (amide III), and 700 (amide V). A pronounced shoulder at 1260 cm^{-1} is a critical feature to distinguish silk II from random coil/silk I in cast silk films treated with methanol. In the FTIR spectra for silk fibroin LB films we have identified this shoulder at 1258 cm^{-1} . This confirms that at least part of the silk fibroin has a silk II conformation.

The explanation for the dominance of a silk II structure in these thin films may be in the mechanical forces present during the application of the solubilized fibroin to the surface of the trough, during compression of the surface of the trough, and/or during transfer of the silk fibroin. During application of the solubilized silk to the surface of the trough with the Pasteur pipet, some shear may induce, in part, a silk II conformation. The silk II conformation, due to its insolubility in the aqueous subphase, would

therefore form the thin film. Another possible source of mechanical shear is the stretching of silk fibroin during transfer and deposition on solid supports. Once a silk fibroin film is formed there may be resistance to transfer and deposition by interchain forces between the polymer chains. The energy needed to break these interchain forces may contribute to the phase transition of the deposited material.

Figure 2 is a TEM of a single layer of the LB silk fibroin film formed at 24°C. The edge of the TEM grid appears in the micrograph as the black areas at the upper and lower corners, while the dark areas in the field are assumed to be thicker regions of the film. The clear or spherical areas in the micrograph are holes in the film. These holes appear irregularly throughout the film as do the thicker regions, and may arise during film drying on the TEM grid. This conclusion is supported by the ellipsometry data which would not be consistent if holes were uniform throughout the film. The physical appearance of the film is affected by the drying and processing conditions. Figure 3 is a micrograph of a silk fibroin LB film where the temperature of the subphase was elevated to 45°C. The physical appearance of the film is different from that seen in Figure 2. The film has striations throughout. The small dark cubic shapes in the film we believe are crystals of LiBr, not removed during the dialysis process, precipitating out of the solution at the elevated temperature. Altering the temperature of the subphase imparts significant changes in the physical appearance of the silk fibroin film. Further studies are underway to correlate the physical environment of the subphase and drying conditions of transferred films with the structure of the LB silk film formed.

Figure 4 shows a micrograph of an electron diffraction pattern of an LB silk fibroin film. The electron diffraction pattern is typical of a polycrystalline material which is characteristic of silk. Minoura et al. (22) and Magoshi et al. (23) have published X-ray diffraction data on cast silk thick films which have similar patterns as those observed here for the LB silk fibroin film. Asakura et al. (26) and Minoura et al. (22), using X-ray diffraction, observed that the preparation and physical treatment of silk films are critical factors in determining whether silk I or silk II structures form. We have yet to confirm with electron diffraction whether the LB silk film is silk I or silk II. Further work is underway to utilize electron diffraction to determine the structure of silk in the films.

Based on the IR data discussed earlier, we expect a silk II conformation to be confirmed for the conditions under which these films were prepared. to determine the conformation characteristic of the LB silk film individual reflections within the electron diffraction pattern would be critical for structure identification. Reflections with d spacings of 9.70, 4.69, and 4.30 Å would indicate a silk II conformation while reflections at 7.25 and 4.50 Å would be indicative of a silk I conformation. Under the appropriate conditions, using the Langmuir method, it may be possible to obtain a well oriented silk I film. This would provide a unique opportunity to experimentally characterize the silk I structure since this structure has eluded definitive structural characterization due to its metastable state.

Table I. Ellipsometry data on silk fibroin LB films deposited on frosted glass slides

Film Characteristic	Number of Layers		
	3	5	7
Multi-Layer Thickness Å	37	65	94
Calculated Monolayer Thickness Å	12.3	13	13.4

Reproduced from *Mater. Res. Soc. Symp. Proc.* 1993 292, 181.

Table II. Comparison of FTIR wavenumbers reported for cast films [17,18] (silk I, silk II) versus those obtained for silk fibroin LB films

Absorption Bands	Cast Membranes		Silk Fibroin LB Films
	Silk I	Silk II	
Amide I	1650	1625	1624
Amide II	1535	1528	1522
Amide III	1235	1260	1258
Amide V	650	700	700

Reproduced from *Mater. Res. Soc. Symp. Proc.* 1993 292, 181.

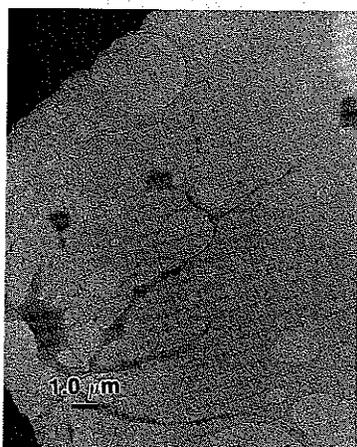


Figure 2. A transmission electron micrograph of the deposited silk fibroin LB film at 24°C. Reproduced from *Mater. Res. Soc. Symp. Proc.* 1993 292, 181.

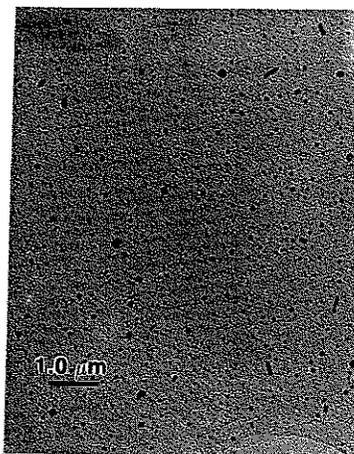


Figure 3. A transmission electron micrograph of the deposited silk fibroin LB film at 45°C. Reproduced from *Mater. Res. Soc. Symp. Proc.* 1993 292, 181.

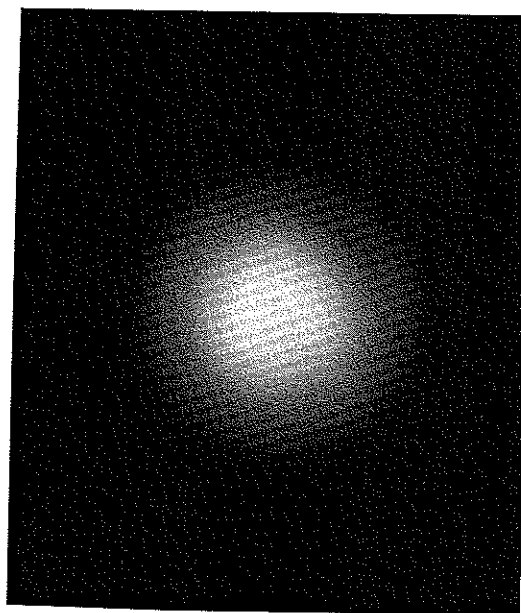


Figure 4. Electron diffraction pattern of silk fibroin LB film. Reproduced from *Mater. Res. Soc. Symp. Proc.* 1993 292, 181.

Acknowledgments

We thank Marian Goldsmith (University of Rhode Island, Kingston, R.I.) for supplying the silkworm cocoons, Abe King and Sam Cohen (Natick) for the TEM analysis and helpful discussions, Aaron Bluhm (Natick) for the FTIR analysis, and Tony Chen (University of Massachusetts, Lowell, MA) for the ellipsometry analysis.

Literature Cited

1. Kuzuhara, A.; Asakura, T., Tomoda, R., Matsunaga, T. *J. Biotechnol.* **1987**, *5*, 199.
2. Asakura, T.; Yoshimizu, H., Kuzuhara, A., Matsunaga, T.J., *J. Seric. Sci. Jpn.* **1988**, *57*, 203.
3. Demura, M.; Asakura, T. *Biotechnol. Bioeng.* **1989**, *33*, 598.
4. Demura, M.; Asakura, T., Kurso, T. *Biosensors* **1989**, *4*, 361.
5. Demura, M.; Asakura, T., Nakamura, E., Tamura, H. *J. Biotechnol.* **1989**, *10*, 113.
6. Izuka, E. *J. Appl. Poly. Sci.* **1985**, *41*, 163.
7. Robson, R.M. *Fiber Chemistry Handbook of Science and Technology*, Marcel Dekker, Inc: New York, N Y, 1985; Vol. IV, pp 647-699.
8. Asakura, T.; Kanetake, J., Demura, M. *Poly-Plast. Technol. Eng.* **1989**, *28*, 453.
9. Yoshimizu, H.; Asakura, T. *J. Appl. Poly. Sci.* **1990**, *40*, 127.
10. Magoshi, J.; Magoshi, Y., Nakamura, S. *J. Poly. Sci., Appl. Polym. Symp.* **1985**, *41*, 187.
11. Kaplan, D.L.; Lombardi, S.J., Muller, W.S., Fossey, S. In *Biomaterials Novel Materials from Biological Sources*, Byrom D., Ed.; Stockton Press, New York, NY, 1991, pp 3-53.
12. Lucas, F.; Shaw, J.T.B., Smith, S.G., *Adv. Prot. Chem.*, **1958**, *13*, 107.
13. Lucas, F. *Nature* **1966**, *210*, 952.
14. Otterburn, M.S. In *Chemistry of Natural Protein Fibers*, Asquith R.S., Plenum Press, New York, NY, 1977, pp 53-80.
15. Minoura, N.; Tsukada, M., Masanobu, N. *Biomaterials* **1990**, *11*, 430.
16. Swart, R.M., *Langmuir-Blodgett Films*, Roberts, G., Plenum Press, New York, NY, 1990, pp 273-307.
17. Marsh R.E.; Corey R.B., Pauling, L. *Biochim. Biophysics Acta* **1955**, *16*, 1.
18. Fossey, S.A.; Nemethy, G., Gibson, K.D., Scheraga, H.A. *Biopolymers* **1991**, *31*, 1529.
19. Magoshi, J. *Kobunshi Ronbunshu* **1974**, *31*, 765.
20. Ishida, M.; Asakura, T., Yokoi, M., Saito, H. *Macromolecules* **1990**, *23*, 88.
21. Magoshi J.; Mogoshi, Y., Nakamura, S. *J. Appl. Poly. Sci., Appl. Poly. Sym.* **1985**, *41*, 187.
22. Minoura, N.; Masuhiro, T., Masanobu, N. *Polymer* **1990**, *31*, 265.

23. Magoshi, J.; Kamiyama, S., Nakamura, S. *Proceedings of th 7th International Wool Textile Research Conference*, 1985, 1, 337.
24. Lotz, B.; Keith, H.D. *J. Mol. Biol.* 1971, 61, 201.
25. Yoshimizu, H.; Asakura, T. *J. Appl. Poly. Sci.* 1990, 40, 1745.
26. Asakura, T.; Kuzuhara, A., Tabeta, R., Saito, H. *Macromolecules* 1985, 18, 1841.

RECEIVED June 29, 1993

U OF MASS AMHERST LIBRARY